Development of an Inertial and Cold Trap Filter For Carbon Fines Management

Juan H. Agui[1] and Robert D. Green[2]
NASA Glenn Research Center, Cleveland, OH, 44135

and

Gordon M. Berger[3]
USRA, Cleveland, OH 44135

The Plasma Pyrolysis Assembly (PPA) is a methane processing technology that integrates with the Sabatier Reactor Assembly (SRA) to further advance oxygen loop closure for spaceflight. A problematic reaction byproduct of the PPA is very fine carbon dust which accumulates on the walls of the reactor and migrates to downstream Environmental Control and Life Support System (ECLSS) components with the effluent flow. The reactor is regenerated periodically by generating a CO_2 plasma within the reactor to clean the internal walls and microwave stub. To address the flow of carbon dust to downstream components, the PPA will require an effective carbon capture management system. While various methods have been attempted through prototype testing, the effective filtering and regenerative performance of these devices remains a challenge. A new approach is being explored which will provide large carbon dust holding capacity by flow inertial impaction and recirculation and low temperature particle quenching techniques. The technique involves a custom-designed housing to produce a strong and large recirculating pattern to remove the dust through inertial forces and confine it to a large collection cup. The collection cup is enshrouded in a cold trap to quench the PPA effluent and enhance precipitation of the remaining carbon from the reaction. The flow then passes through a single stage baffle and tube filters before exiting through the outlet at the top of the housing. A prototype of this concept was built and is being tested with simulant dust. This report will highlight the design and operation of the prototype and provide preliminary test results.

Nomenclature

AES	=	Advanced Exploration Systems
CM	=	crew member
ECLSS	=	Environmental Control and Life Support Systems
g	=	Earth gravity (9.8 m/s^2)
ISO	=	International Organization for Standardization
LSS	=	Life Support System
MSFC	=	Marshall Space Flight Center
p	=	pressure
PPA	=	Plasma Pyrolysis Assembly
SLPM	=	standard liters per minute
SRA	=	Sabatier Reactor Assembly
STD	=	standard deviation
TC	=	thermocouple
κ-ω	=	Two-equation turbulence model

[1] Aerospace Engineer, Thermal Systems and Transport Processes Branch, 21000 Brookpark Rd/Mail Stop 77-5.
[2] Aerospace Engineer, Thermal Systems and Transport Processes Branch, 21000 Brookpark Rd/Mail Stop 77-5.
[3] Research Scientist, Low-Gravity Exploration Technology Branch, 21000 Brookpark Rd/Mail Stop 110-3

I. Introduction

The Plasma Pyrolysis Assembly (PPA) is a methane processing technology that integrates with the Sabatier Reactor Assembly (SRA) to further advance oxygen loop closure for spaceflight. Use of the PPA could enable the theoretical recovery of > 86% of the oxygen from the CO_2 produced on the ISS.[1] The PPA decomposes the methane produced from the reaction of CO_2 with hydrogen in the Sabatier reactor into hydrogen and various hydrocarbons: mainly acetylene, and smaller quantities of unconverted methane, ethylene, and ethane. The kinetics of the thermal decomposition can be found in Ref. 2. In addition, solid carbon particles are generated at a small constant rate in the plasma and subsequently collects on surfaces. The carbon particles formed are physically very small, with sizes as small as 100 to 200 nm[3]. If not mitigated the carbon dust load could eventually foul the PPA reactor and downstream Environmental Control and Life Support Systems (ECLSS) subsystems, limiting and interrupting the air revitalization system.

Reference 4 provides a chemical model of carbon particle formation during pyrolysis. In this model the gaseous hydrocarbon initially forms macromolecules which then nucleate and grow into liquid droplets before the carbon particle is pyrolyzed. While this process mainly takes place in the reaction chamber of the PPA, the effluent from the PPA still contains small quantities of unreacted methane which could continue to decompose into acetylene and carbon. Quenching of the effluent can be used to stop further decomposition of the unreacted methane and precipitate the remaining precursor carbon particles.

Several filter technologies have been assessed through prototype testing for their effectiveness in containing the carbon particulates produced by the PPA.[5,6] Most of these methods used more conventional media filtration techniques with high capturing capacity of the carbon dust. Although some success has been achieved through these trials, including filter regeneration concepts, an effective method of carbon removal remains a gap in the full implementation of the PPA technology. The main challenge that remains is the continuous operation of the filter system for extended operating periods. Under nominal operation, the PPA generates on average 40 mg/hr (see Ref. 3) of solid carbon with short maintenance periods, of the order of 15 minutes, to regenerate PPA reactor chamber due to carbon build up on the internal walls and the microwave stub. A CO_2 plasma is generated to essentially burn off (or oxidize) the carbon from these surfaces. The accumulation of this rate of carbon generation for a 1000-day mission (i.e., a notional Mars transit mission) will require an effective low maintenance and virtually continuously filtering system.

In this paper, a new carbon trap filter concept is presented. Particles are collected through filtration and separation concepts, while also implementing a cold plate to accelerate the quenching and collection of the carbon onto a cold collection cup. Details of the design, modeling results and preliminary testing is presented.

II. Filtration and Carbon Capture Mechanisms

The carbon trap filter was designed to trap the solid carbon through various capturing mechanisms. These include inertial separation, flow recirculation, flow tortuosity, media filtration, and particle quenching. The schematic of the concept is presented in Figure 1. The gaseous stream containing the carbon, in particle and droplet form, enters through the inlet tube of the filter, at the top of the filter housing. The flow enters at a high velocity at the full-scale PPA flowrate, with velocities of up to 2 m/s for a 4 crewmember (4-CM) flow rate and a 2.54 cm diameter inlet tube. The axial inlet tube is extended down towards the bottom of the collection cup, where the high-speed stream meets the sudden perpendicular bottom wall inducing a stagnation flow. The prototype described in a subsequent section (section IV) has a conical bottom wall cavity instead of a flat bottom wall. Large particles inertially separate from the flow and impinge onto the bottom wall at the stagnation point. As depicted in Fig. 1, the partial enclosure of the collection cup, except for an axis-symmetric slit connecting it to the upper chamber, causes a strong recirculation bubble to form in the collection cup, increasing the residence time of the gaseous particle-laden stream there. The vortical motion of the recirculation bubble also has the effect of spinning the large particles out towards the walls of the collection cup. The collection cup is cooled in order to quench the PPA effluent, hindering further decomposition of the effluent products and any further carbon particle generation, and precipitating the remaining carbon from the initial plasma reaction. The extended residence time brought about by the recirculating flow in the collection cup has the added effect of further quenching the stream. Only small particles that are entrained sufficiently by the flow make it through the slit between the collection cup and on to the upper chamber. The prototype, to be described later, has long slender channel instead of a simple slit opening which makes the flow path more tortuous towards the upper chamber. On the top wall of the upper chamber, an array of tubular filters collect the remaining particles before the gaseous stream exits.

The performance of the filter system can be adapted through various adjustments, set points, and use of different filter media on the last stage of filtration. First, the distance between the tip of the inlet tube to the bottom plate will affect the level of stagnation flow and the strength of the recirculation zone in the collection cup. The slit size opening

at mid-height determines the size of particles that pass through to the upper chamber. The set temperature on the collection cup will alter the amount of thermal quenching of the PPA effluent. Also, the media used on the tube filters will affect the amount of particle penetration, pressure drop, and the holding capacity of the smallest particles that pass to the upper chamber. Lastly, the collection cup and upper chamber can be sized with sufficient capacity to last a full mission.

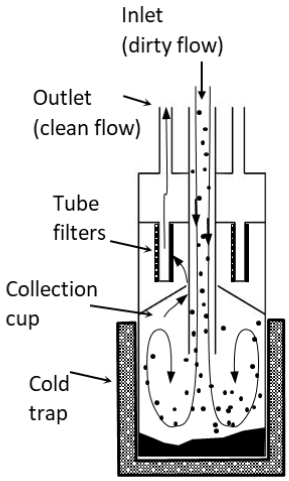

Figure 1: Schematic of carbon cold trap filter concept.

III. Modeling

Computational Fluid Dynamics (CFD) and particle tracing modeling performed through COMSOL Multiphysics software was used to aid the design process and assess the performance of the carbon cold trap filter under nominal operating conditions. A 3D 60° sector geometry was generated in a CAD program and imported into COMSOL. The boundary conditions are labeled in Fig. 2a. The 60° sector was chosen to represent 6 tube filters placed in a circular pattern on the top plate of the filter housing. Baffle walls are included at mid-height connecting the lower collection cup chamber and the upper chamber. Also, thermal fins were constructed on the bottom conical wall of the cup to increase surface area and enhance particle collection. The geometry was gridded as shown in Fig. 2. The grid contains over 300,000 elements consisting mainly of tetrahedral elements. Hydrogen gas properties were used to represent the main PPA effluent constituent, and the gravity force was turned off.

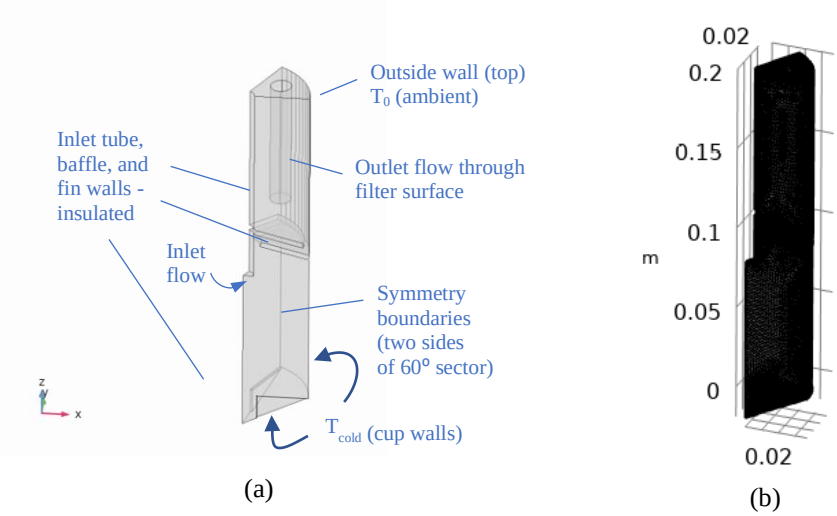

Figure 2: COMSOL model (a) geometry with boundary condition labels, (b) gridded geometry

A steady-state Reynolds Averaged Navier-Stokes (RANS) solver employing the two-equation κ-ω turbulent closure model (developed by Wilcox[7]) was used to obtain the flow and pressure field in the flow domain. The flow volume was initialized at ambient temperature (i.e., 293 K) and at the nominal PPA operating pressure of 100 torr (13332 Pa). The velocity contours plotted on an axial cut plane in Fig. 3 provide a visual aid of the flow development. The flow which enters the collection cup volume at a temperature of 50 °C above the initialized temperature (to arbitrarily represent the warmer product stream from the PPA reactor) and at close to 2 m/s, impinges the central apex of the conical cavity and then turns laterally toward the outer wall. The recirculation bubble is discernable above the bottom surface of the filter. In the mid-height a slender serpentine channel can be seen where the flow is accelerated before entering the upper chamber. Subsequently, the flow is directed upwards and surrounds the tube filter. The pressure contour in Fig. 3b shows the differences in pressure between the collection cup (lower chamber) and the upper chamber of the filter. The pressure difference between the two chambers was found to be very small. It should be noted that this result did not account for the pressure drop across the tube filters which can be expected to be of the order of hundreds of pascals.

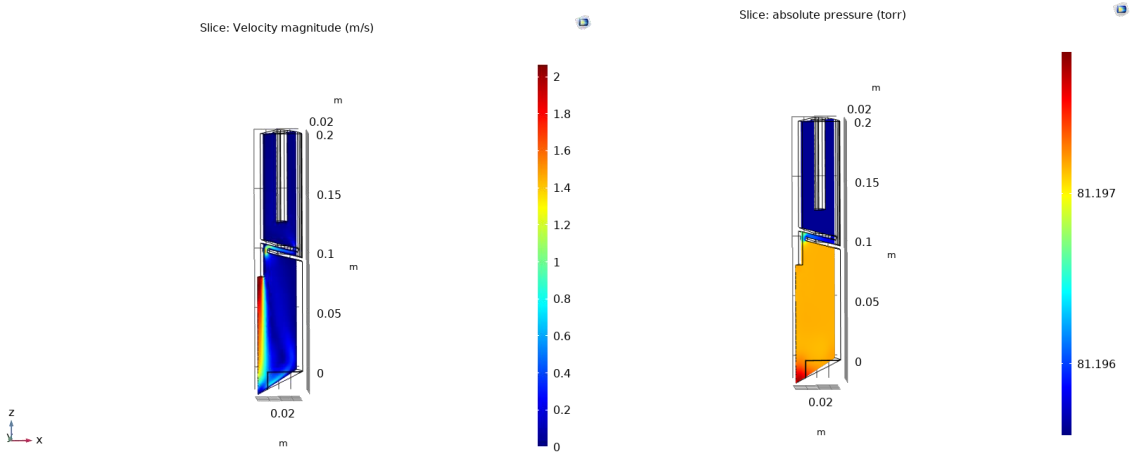

Figure 3: Modeling results (a) velocity contour, (b) pressure contour.

Once the flow and temperature fields were established in COMSOL, the software's Particle Tracing module was used to investigate the particle trajectories. With the Particle Tracing module, the individual particle's material properties (i.e., density, particle diameter) and drag and other forces (e.g., thermophoretic forces) are modeled. In the present simulations, the particles were modeled as spherical particles with a specific density of 2.2 g/cm^3, i.e. the specific density of solid carbon. A group of particles are released at t = 0 into the flow domain at the tip of the inlet tube. The particle injection consisted of uniformly distributed particles from 1 μm to 20 μm. This range of particle sizes were thought to be appropriate to show the size dependence on the fate of particles reaching different and successive sections of the filter due to the different capturing mechanisms. The Particle Tracing model was run as an unsteady solver which provided histories of the particle trajectories. Figure 4 shows the particle trajectories at incremental physical time steps.

The Particle Tracing module was used to visualize the fate of the particles inside the filter geometry based on their size. Particularly, the simulations were instructive in showing the general separation performance of the filter, although the effect of particle shape could not be modeled. A color map of particle sizes is provided in the figure. At 0.15 seconds the splashing effect of the particles on the bottom conical wall can be seen. At 0.5 seconds and 1.0 second the development of the particle circulation flow is discernable. Also, at the 1.0 second mark small particles can be seen migrating to the upper chamber. These particles reach the surface of the tube filter around the 2.0 second mark. Lastly, at 5.0 seconds the effect of size segregation can be seen where most of the large particles remained dispersed in the collection cup, while the smallest particles, under 9 μm or 10 μ, end up on the tube filter surface. An appropriate particle filter can be used here in the upper chamber to capture these smallest particles. The model did not account for the quenching effect on particle capture on cold surfaces.

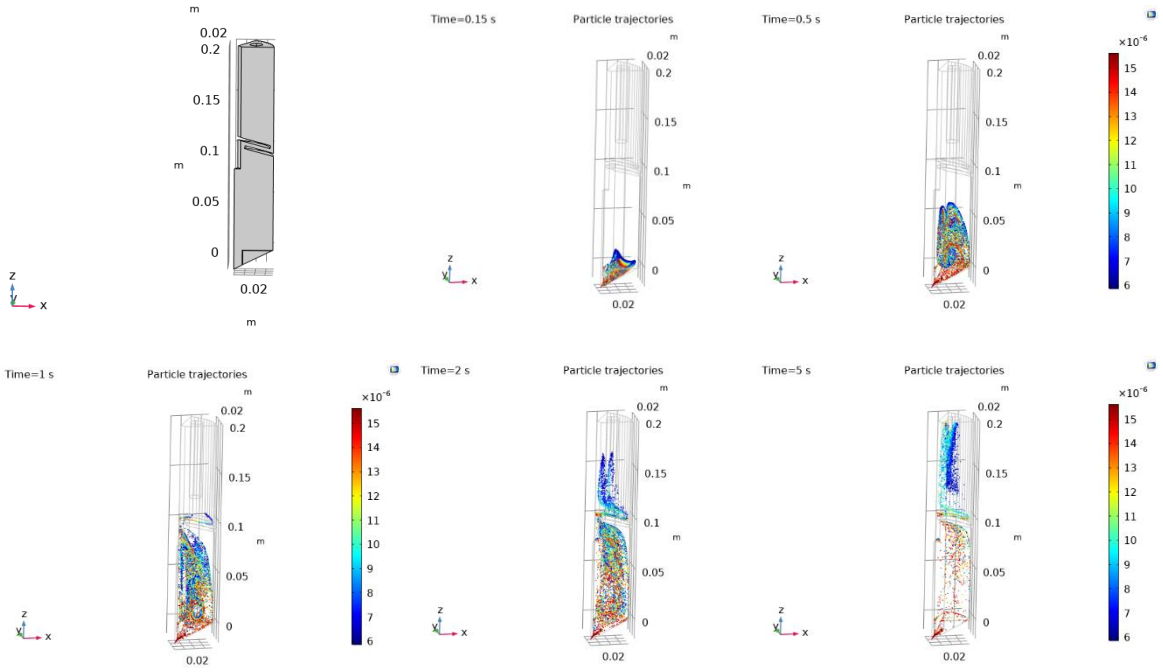

Figure 4: Modeling results: Time sequence of particle tracing

In addition, thermal modeling through COMSOL's Heat Transfer module was performed by applying a lower and constant temperature on the collection cup walls. Figure 5 shows the temperature contours along an axial cross-section of the flow domain. In Fig. 5a, only the bottom wall of the collection cup was maintained at the lower temperature, while both the bottom and side walls were maintained at the lower temperature in Fig. 5b. These plots show that in the case of the bottom and side wall cooling (Fig. 5b) the temperature of the gas is generally cooler in the collection cup, particularly in the zone near the side wall. Specifically, in this case, the temperature was ~ 5 ºC lower in the recirculation zone (circular shape contour near the bottom plate seen in Fig. 5b) and ~ 15 ºC lower in the region adjacent to the side wall. These data indicate that both the bottom and side walls should be cooled to more extensively cool the gas phase in the collection cup. This will maximize the quenching of the incoming gas containing the nucleated carbon particles.

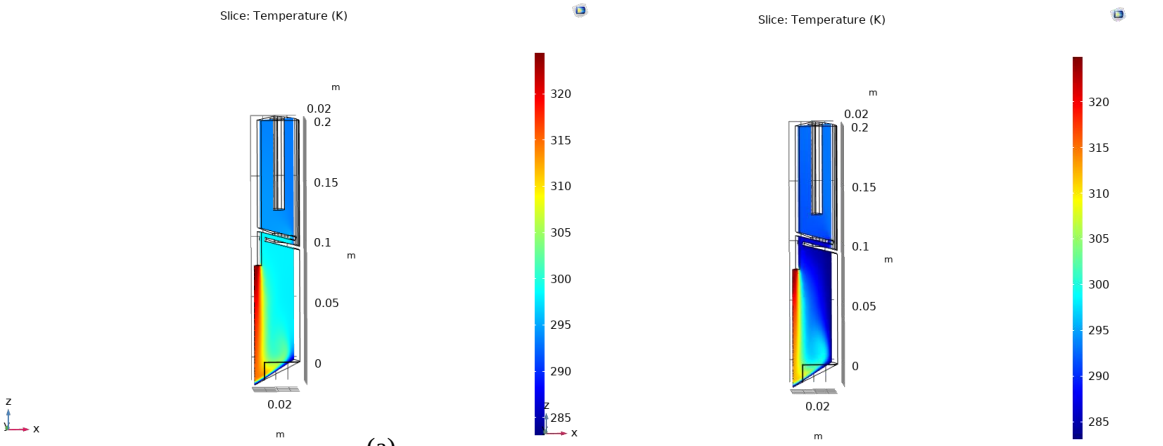

(a) (b)

Figure 5: Modeling results: Temperature contours

IV. Experimental Setup

An experimental prototype of the cold trap filter concept was tested in the laboratory to gain some ground-based performance data. A picture of the experimental setup is shown in Figure 1. The cold trap filter prototype is located in the center of the setup. An inlet HEPA filter is used to introduce particle free air flow into the filter system. The flowrate was set by a mass flow controller before the inlet. Four thermoelectric coolers were mounted on the outside of the aluminum collection cup to bring down the temperature. Three were placed on the side walls separated at 120° circumferentially around the outside of the round collection cup, and a fourth thermoelectric cooler was mounted underneath the bottom wall of the collection cup. A fixed voltage power supply was used to power the thermoelectric coolers, and the connection to the power supply was controlled by a thermostat that maintained the nominal set temperature on the collection cup. Four type-K thermocouples were mounted onto the outside wall of the collection cup. Three were mounted on the side walls of the collection cup centered between adjacent thermoelectric coolers, and the fourth thermocouple was mounted on the bottom wall adjacent to the fourth thermoelectric cooler. A semi-conductor based differential pressure transducer measured the pressure drop across the filter system, i.e., between the inlet tube and downstream of the manifold at the exit of the filter system. Two different sets and types of tube filters (not visible in Fig. 6) were used in testing. One set consisted of porous metal tube filters with a 10-micron rating. Despite the 10 μm rating, the type of porous metal filter chosen can readily capture particles smaller than 10 μm through the process of depth filtration under low flow conditions. Another set of filters consisted of using commercial inline media filter cartridges rated at 98% efficiency.

The outlet plumbing of the four tube filters were coupled to a manifold which was connected to a scroll pump. The scroll pump was used to generate the flow at the nominal PPA operating pressure of 100 torr. A needle valve installed upstream of the inlet HEPA filter was used to control the flowrate through the pump at the PPA pressure.

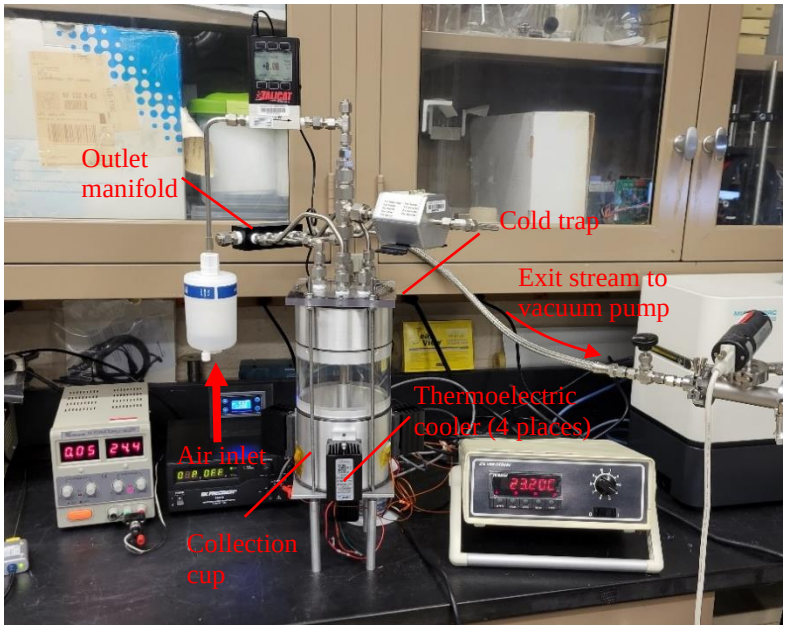

Figure 6: Experimental setup

In another setup, the carbon trap filter was slightly reconfigured to perform a dust challenge test. A commercial particle generator was used to introduce the challenge dust, in this case ISO Fine Test Dust, through the inlet tube. To perform this a co-flow was set up in the main axial inlet tube by inserting a smaller diameter tube (12.7 mm diameter), which was connected to the particle generator on the other end, down through the center of the 2.54 cm diameter inlet tube. The clear Lexan cylindrical wall in the middle of the carbon trap housing and a Lexan plate on the top of the filter allowed for viewing of the dust loading in the collection cup and upper chamber respectively.

V. Results

Once the prototype was assembled a leak test was performed to ensure the filter housing was leak tight. Flow tests were then performed with the activated thermoelectric coolers to determine the pressure drop and temperature uniformity on the collection cup. The activation of the thermoelectric coolers was controlled by laboratory grade thermostat to achieve different set temperatures on the collection cup. The power to the thermoelectric cooler was monitored and found to be steady at around 23 Watts (~ 6 Watts per cooler) for all tests during the transition to different set temperatures.

The main differences between the experimental prototype and the COMSOL model are the use of air as the constituent gas, the more acute angular conical cavity (60° half conic angle vs. 30°), 1-g gravity force, and the use of only four tube filters. Also, the inline filters and porous metal tube filters used in these tests contributed to the higher pressure drop values across the whole filter system as compared to the modeling results (which did not account for the tube filters).

The following sections present the pressure drop data for a range of flowrates, a limited point temperature mapping of the collection cup using four thermocouples, and the results of a dust challenge test.

A. Pressure drop

The pressure drop was measured under a range of flowrates at the nominal PPA reactor pressure of 100 torr. In these preliminary tests room air was used instead of the acetylene and hydrogen mix that actually exits the PPA. Figure 7 shows the pressure drop vs flowrate at various collection cup wall temperatures.

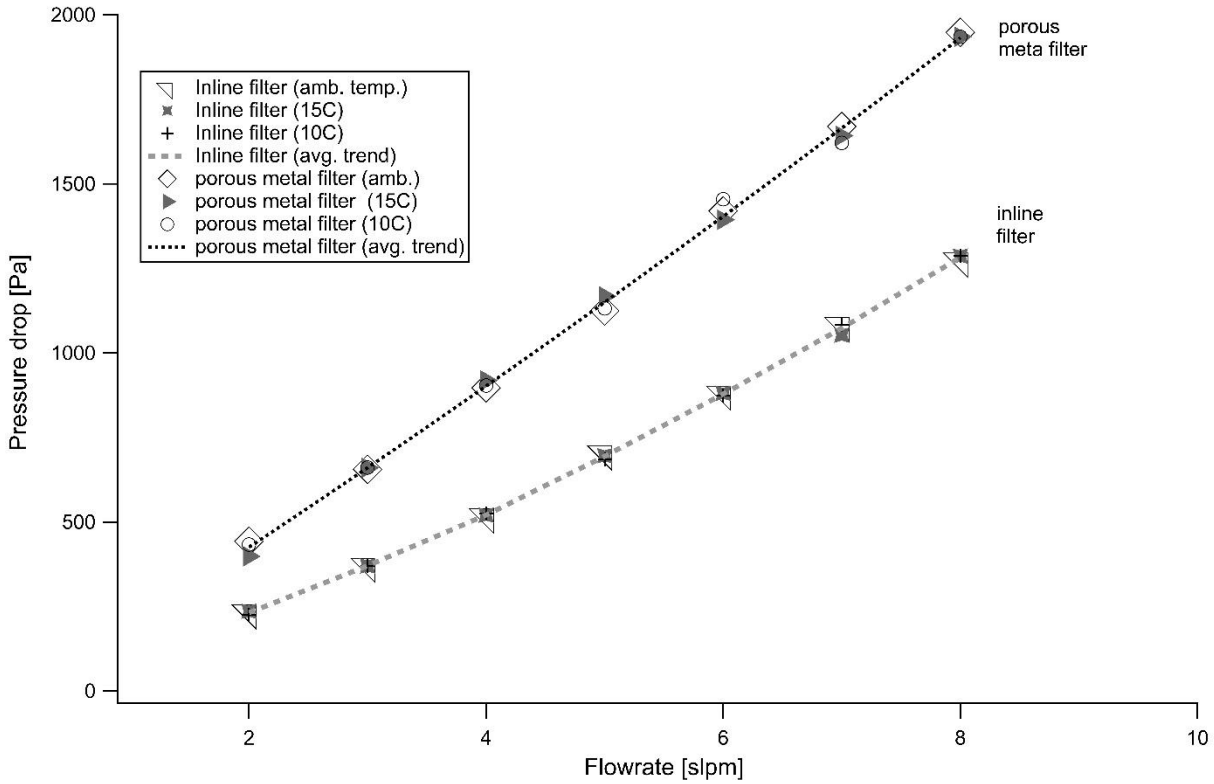

Figure 7: Pressure drop as a function of flow rate at various collection cup temperature - HEPA tube filters

The plots at each of the three temperatures, in either the inline filter or porous metal filter case, were very close in value, indicating that the temperature of the flow had no effect on the hydrodynamic performance of the overall filter system. In the inline filter case, the pressure drop appears to have a slight non-linearity, where the slope of the pressure drop curve increases with flowrate, while for the porous metal filter the rise is nearly linear. This may have something to do with the design of the inline filter which has a small diameter axial inlet which is much more restrictive than the large permeable surface area of the tubular porous metal filter. In the inline filter case, the average pressure drop rise with flow rate was found to be 175 Pa/slpm over the range of flowrates from 1 to 8 slpm. The average pressure drop

rise for the porous metal filter was found to be significantly higher with a rise of 252 Pa/slpm. It should be noted that the pressure drop was taken between the inlet tube, at a distance of about 100 mm upstream from the inlet tube tip, and the exit tubing from the outlet manifold. Therefore, the pressure drops reported incorporate the pressure head losses between the lower and upper chambers of the filter, the pressure drop across the inline or porous metal tube filters, as well as the losses through the manifold and tubing connections and fitting.

The overall pressure drop of the system using the inline filters ranged from ~ 230 Pa at the 1 slpm flowrate to approximately 1270 Pa at the 8 slpm flowrate with the inline filters, the latter being approximately equivalent to 4-CM flow rate. The pressure drop produced with the metal porous filter ranged from ~ 440 Pa at 1 slpm to ~ 1900 Pa at 8 slpm.

B. Temperature uniformity

Table 1 presents the measured temperatures obtained during each of the tests taken at the three nominal collection cup temperatures. Prior to testing, a check of the temperature variation between thermocouples was performed with the four thermocouples immersed in a bath of ice water. Each of the thermocouple temperatures were found to vary slightly from the reference 0 °C, for an overall variation of about 2.1 °C. During testing, the temperatures also appeared to be offset by the similar amounts. To compensate for this, the zero value for each thermocouple was adjusted to match the 0 °C reference temperature. For the test setup, three thermocouples, TC1-TC3, were distributed circumferentially around the side walls of the collection cup centered between adjacent thermoelectric coolers. The fourth thermocouple, TC4, was mounted underneath the bottom plate. The tips of the thermocouples were mounted flush with the walls of the collection cup, and secured there with a piece of foam insulation and a strip of tape. When the set temperature was reached the thermostat automatically deactivated the thermoelectric coolers, and a set of pressure drop reading were taken at different flowrate settings. The temperatures given in Table 1 represent a time average of the temperatures taken during each flowrate setting at the set nominal temperature. Because of the duration of the tests while sweeping through the range of flowrates at the lower temperatures, the thermoelectric coolers cycled on and off causing the temperature of the collection cup to drift a few degrees between the internally programmed upper and lower set points on the thermostat.

The temperatures were found to be generally uniform around the collection cup with small variations. The inline filters and porous metal filters produced about the same variations in temperature. The measured temperature ranges (i.e. maximum minus minimum) for the four thermocouples were found to be within 1.85 °C for the inline filters, and within 2.2 °C for the porous metal filter. It should be noted that the accuracy of thermocouples is typically around 2 °C. Correspondingly, the standard deviation of the four spatially distributed temperatures was found to be within 0.83 °C for for the inline filters, and within 0.92 °C for the porous metal filters. These similar temperature variations took place despite that fact that there was active cooling at the two lowest nominal temperatures and no cooling at the highest nominal temperature. In general, these results indicate that the arrangement of the four thermoelectric coolers can provide fairly uniform temperatures around the collection cup. The results of the COMSOL model also indicated that the interior flow domain in the collection cup was generally cooler when both the side and bottom walls of the collection were cooled, indicating that the four thermoelectric cooler configuration is a suitable arrangement for thermal control.

Table 1: Temperature on the collection cup at various nominal temperatures

Filter	Nominal temperature	TC1	TC2	TC3	TC4	range	STD
	°C	°C	°C	°C	°C	°C	°C
Inline	10	10.30	10.82	10.12	11.97	1.85	0.83
Inline	15	14.83	15.62	14.60	15.63	1.03	0.53
Inline	22	23.42	23.41	21.68	22.54	1.73	0.83
Porous metal	10	10.17	10.72	10.33	11.83	1.66	0.75
Porous metal	15	15.04	15.50	14.18	16.38	2.20	0.92
Porous metal	22	21.47	21.48	19.89	20.64	1.59	0.76

C. Dust challenge

Preliminary results of a dust challenge test using ISO Fine Test Dust were also obtained. Qualitative visual results of where the particles were collected in the different chambers and sections of the filter system are shown in Fig. 8. Figure 8a shows the deposition of the dust in the collection cup. The bottom of the inlet tube and the thermal fins on the bottom of the collection cup are visible. The dust deposition is discernable and appears to be appreciable. Figure 8b shows an image in the upper chamber. Only minor deposition was noticed in this chamber. These results qualitatively give an indication that the filter concept appears to perform as expected.

(a) (b)

Figure 8: Pictures after dust challenge test (a) collection cup, (b) upper chamber.

VI. Conclusion

This paper presents a cold trap filter concept for PPA carbon fines management. The details of the concept and prototype design were presented. CFD, heat transfer, and particle tracing modeling were used to aid in the design and lay a basis of performance expectations. The modeling showed how the different particle capturing mechanism, through filtration and separation, affected the transport of the particles through the different stages of filtration of the filter system. Particles > 10 µm tended to collect in the collection cup, while particles < 10 µm made it to the upper chamber where an array of tube filters would capture the remaining particles. The modeling also confirmed that active cooling would be needed on both the side and bottom walls of the collection cup for more extensively cooler temperatures of the gas-phase in the collection cup. The experimental data showed that the pressure drop increased slightly non-linearly with flow rate with the inline media filter and nearly linearly with the porous metal tube filter. The maximum pressure drops were 1270 Pa and 1900 Pa respectively for the inline filter and porous metal fiter cases at the 8 slpm flowrate. The data also showed that the temperature on the collection cup walls could be kept nearly uniform by using a four thermoelectric cooler configuration. A dust challenge test showed qualitatively that the filter concept appeared to perform as expected. Future work will consist of more extensive testing of the prototype, particular particle challenge test to determine capturing efficiency. Integrated testing of the cold trap filter with the PPA at the NASA Marshall Space Flight Center (MSFC) will also be planned.

Acknowledgments

The support from NASA's Life Support System (LSS) project under the Advanced Exploration Systems (AES) program is greatly appreciated. The authors would also like to thank Mr. Daniel Gotti (USRA) for the design of the Cold Trap Carbon Filter.

References

[1]Greenwood, Z., Abney, M., Stanley, C., Brown, B. and Fox, E., 2018, July. State of NASA Oxygen Recovery. 48th International Conference on Environmental Systems.

[2]Green, R.D., Meyer, M.E., Agui, J.H., Berger, G.M., Vijayakumar, R., Abney, M.B. and Greenwood, Z., 2015, July. Characterization of carbon particulates in the exit flow of a Plasma Pyrolysis Assembly (PPA) reactor. 45th International Conference on Environmental Systems.

[3]Wheeler, R.R., Hadley, N.M., Wambolt, S.R. and Abney, M.B., 2014, July. Third generation advanced PPA development. 44th International Conference on Environmental Systems.

[4]Lahaye, J.G.J.B., Prado, G. and Donnet, J.B., 1974. Nucleation and growth of carbon black particles during thermal decomposition of benzene. Carbon, 12(1), pp.27-35.

[5]Agui, J., Green, R., Vijayakumar, R., Berger, G., Greenwood, Z., Abney, M. and Peterson, E., 2016, July. Filtration of carbon particulate emissions from a Plasma Pyrolysis Assembly Reactor. 46th International Conference on Environmental Systems.

[6]Agui, J., Berger, G., Vijayakumar, R., West, P., Mitchell, K., Abney, M. and Greenwood, Z., 2017, July. Particulate Filtration from Emissions of a Plasma Pyrolysis Assembly Reactor Using Regenerable Porous Metal Filters. 47th International Conference on Environmental Systems.

[7]Wilcox, D. C., "Turbulence Modeling for CFD," DCW Industries, Inc., La Canada, CA, 1994